JACS Au
AN OPEN ACCESS JOURNAL OF THE AMERICAN CHEMICAL SOCIETY
pubs.acs.org/jacsau
Article

Unexpected Charge Effects Strengthen π−Stacking Pancake Bonding

Zhong-hua Cui,* Meng-hui Wang, Hans Lischka, and Miklos Kertesz*

Cite This: *JACS Au* 2021, 1, 1647−1655
Read Online

ACCESS | Metrics & More | Article Recommendations | Supporting Information

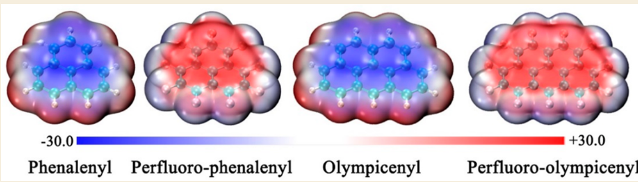

ABSTRACT: Phenalenyls (PLYs) are important synthons in many functional and electronic materials, which often display favorable molecule-to-molecule overlap for electron or hole transport. They also serve as a prototype for π-stacking pancake bonding based on two-electron multicenter bonding (2e/mc). Unexpected near-doubling of the binding energy is obtained for the positively charged PLY_2^+ dimer with an effect similar to that seen for the positively charged olympicenyl (OPY) radical dimer. This charge effect is reversed for the perfluorinated (PF) dimers, and the negatively charged perfluorinated (PF) dimers PF−PLY_2^- and PF-OPY_2^- become strongly bound. Long-range interactions reflect these differences. Also surprising is that in this case the pancake bonding corresponds to single-electron (1e/mc) or a three-electron (3e/mc) multicenter bonding in contrast to the 2e/mc bonding that occurs for the neutral radical dimers. The strong preference for a large intermolecular overlap is maintained in these charged dimers. Importantly, the preference for π-bonding in the charged dimers compared to σ-bonding is strongly enhanced relative to the neutral PLY dimers.

KEYWORDS: *pancake bond, intermolecular interactions, π-stacking, fluorinated phenalenyl dimer, charged π-dimers, MR-AQCC theory*

1. INTRODUCTION

π-Stacking configurations are ubiquitous in aggregates of polycyclic aromatic hydrocarbons (PAHs) and other conjugated molecules and are often driven by ordinary noncovalent van der Waals interactions. A quite unconventional mechanism occurs when multicenter partially covalent electron sharing between conjugated radicals leads to π-stacking, often resulting in highly conducting organic crystals.[1−5] In addition to its importance in conducting organics, this type of intermolecular interaction has increasingly been recognized as a driving force of aggregation among π-conjugated neutral and charged (ionic) radicals.[6−9] Many molecules in this category have exciting optoelectronic and magnetic properties and the potential to exploit unpaired spin densities of the monomers to engineer exceptionally close π−π contacts.[10,11]

This effect has been referred to as "pimerization" or "pancake bonding"[12−21] and occurs when the overlap between the two singly occupied π-molecular orbitals (SOMOs) undergo spin-pairing, creating diamagnetic dimers and larger aggregates. Recent progress both in the experiments and computational modeling have shown that this mechanism is robust and sufficiently widespread. Key features of these unique intermolecular interactions include shorter-than-van der Waals (vdW) contacts[22] and directional atom-over-atom packing geometries in contrast to the atom-over-bond or atom-over-ring packing typical of closed-shell molecules.[12,14] For many applications, it is critical to avoid σ-bond formation so that the highly overlapping π-stacking configuration can be maintained. We shall see momentarily that in addition to avoiding σ-bond formation with bulky side groups,[20] an alternative mechanism is offered by partial charging.

A hitherto unexplained aspect of pancake bonding is the high prevalence of partly charged pancake-bonded dimers, trimers, and other aggregates. Should pancake bonding be strongly affected by introducing charge into a pancake-bonded dimer? In their pioneering study, Small et al.[15] compared the dimerization energy of the neutral and +1 charged dimers of the prototypical pancake bonding molecule, phenalenyl (PLY, **1**). They found through wave function quantum chemistry at the CP-MRMP2/6-31G(d) level that the PLY_2^+ cation radical dimer is bound by 20 kcal/mol in contrast to the neutral dimer, which is bound by only 11 kcal/mol. Given the fact that the former has a formal pancake bond order (PBO, see eq 1) of only 1/2 versus 1 for the latter, they found that while the covalent contribution was reduced and the dispersion interactions remained largely unchanged, the difference was mainly due to an increase of the electrostatic attraction.[15,23] We are expanding these findings by comparing cationic and anionic dimers of PLY and olympicenyl (OPY, **2**) and their perfluorinated derivatives, which are illustrated in Scheme 1.[24] The problem is important because the number of charged pancake-bonded systems is

Received: June 17, 2021
Published: August 5, 2021

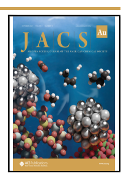

much larger than the number of the neutral ones,[8,9,25−28] as shown by recent examples.[29−32]

Scheme 1. Monomers, Dimer Complexes, and Their Key Parameters Studied in This Work[a]

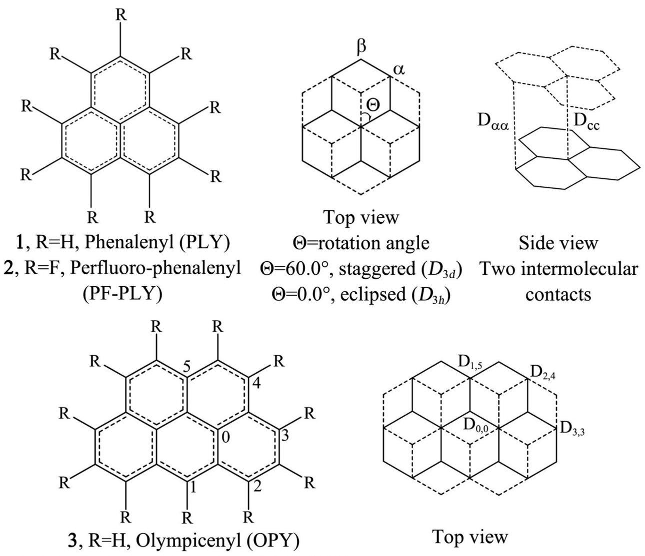

1, R=H, Phenalenyl (PLY)
2, R=F, Perfluoro-phenalenyl (PF-PLY)
3, R=H, Olympicenyl (OPY)
4, R=F, Perfluoro-olympicenyl (PF-OPY)

[a]Notice the atom-over-atom stacking in the dimers, which is indicative of some covalent character in the intermolecular bonding interaction. The PLY_2 dimer displays two-electron 12-center (2*e*/12c) bonding at the D_{3d} symmetry, and the $(OPY)_2$ dimer[21] displays two-electron 20-center (2*e*/20c) bonding at the C_{2h} symmetry. See also Scheme S2.

Scheme 2 illustrates a molecular orbital interaction diagram for PLY and its neutral and charged dimers for the three types of

Scheme 2[a]

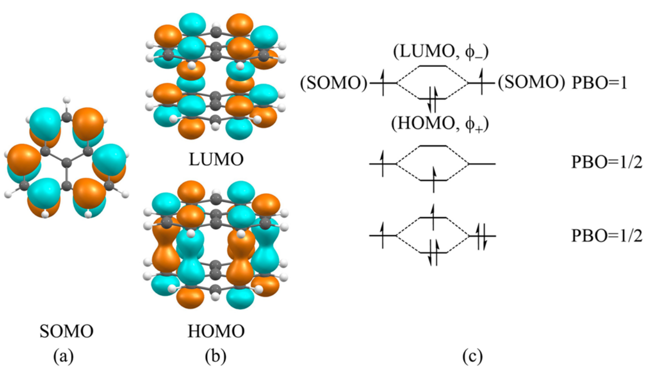

[a](a) Singly occupied molecular orbital of the PLY radical localized on *α*-carbons (Scheme S1 illustrates the SOMO for OPY), (b) bonding and antibonding combination of the two SOMOs in a pancake bonding configuration with a D_{3d} *π*-stacking geometry, and (c) orbital occupancies and formal pancake bond orders (PBOs) of a neutral radical dimer, a dimer cation, and a dimer anion.

pancake bonding under discussion here: two-electron multicenter bonding (2e/mc) with PBO = 1; one-electron multicenter bonding (1e/mc) with PBO = 1/2; and three-electron multicenter bonding (3e/mc), also with PBO = 1/2. Here PBO stands for a formal through space pancake bond order defined as[15]

$$PBO = 1/2(N_{bind} - N_{anti}) \tag{1}$$

where N_{bind} is the number of electrons in the bonding orbitals and N_{anti} is the number of electrons in antibonding orbitals. As a practical matter, only the intermolecular bonding and antibonding orbitals need to be counted.

The main components of the interactions between the two phenalenyls in each dimer are analyzed using dissociation and rotational potential energy surface (PES) scans. Rotational scans are particularly insightful for PLY dimers because the SOMO−SOMO overlap can be turned on (D_{3d}, $\theta = 60°$) or turned off ($\theta = 30°$). Such a simple tool is not available for OPY due to its lower symmetry. Partly for this reason, we also use an energy decomposition analysis (EDA)[33,34] that is applicable regardless of the symmetry. We rely to a large extent on the high-level multireference-averaged coupled cluster (MR-AQCC/6-31G-(d))[35] method, which has been shown to have good performance[36,37] due to the balance for the description of the multireference effects (static electron correlation) induced by the two near-lying orbitals φ_+ and φ_-, as illustrated in Scheme 2, and the dynamic electron correlation responsible for the dispersion-type intermolecular electron correlation energy. Additionally, appropriate DFT computations have been performed.

2. COMPUTATIONAL METHODS

The geometries of the neutral phenalenyl (PLY, **1**) and olympicenyl (OPY, **3**), the perfluoro-phenalenyl (PF−PLY, **2**) and perfluoro-olympicenyl (PF-OPY, **4**) dimers, and their singly charged cationic and anionic analogues were optimized using the (U)M05-2*X*/6-311G(d) level of theory[38] in which the broken-symmetry spin-unrestricted (*U*) formalism was used for the neutral species. All isomers were confirmed as local minima using frequency computations. The geometries of all neutral and singly charged dimers considered here were also fully optimized by MR-AQCC/3-21G for the neutral, +1, and −1 charged dimers of both PLY and PF−PLY. Additionally, the geometries of the neutral, +1, and −1 charged dimers of PLY were also optimized with MR-AQCC using the larger 6-31G(d) basis. Good agreement was found between the results obtained with the two basis sets, which was used as the justification for continuing the MR-AQCC calculations with the computationally much more efficient smaller basis set. Molecular orbitals (MOs) created by the CASSCF method were used in the MR-AQCC calculations with the same CAS(2,2) as used in the CASSCF calculations for the neutral ones,[39] whereas the state-averaged (SA) CAS(1,2) and CAS(3,2) calculations were used for the optimizations of the cationic and anionic species, respectively. MR-AQCC/3-21G was used to compute the rigid rotation and dissociation potential energy scans for all the neutral and charged dimers with further extensive computations using the larger 6-31G(d) basis. The MR-AQCC calculations were performed using the COLUMBUS program suite.[40,41] The unpaired electron population analysis[42,43] was completed using the TheoDORE program.[44,45]

For interpretative purposes, the separation of the different energy terms is highly desirable, especially the separation of the covalent-like bonding interaction due to the SOMO−SOMO overlap that produces the electron delocalization over the dimer versus the vdW interaction, E_{vdW}.

E_{vdW} includes dispersion, Pauli (steric) repulsion, and electrostatic interactions. We found it useful to separate the vdW component (E_{vdW}), from the attractive SOMO−SOMO interaction, ($E_{SOMO-SOMO}$), a term that reflects a covalent-like component of the interaction energy.[39,46] This decomposition, albeit approximate, is useful for two reasons. First, there are no directly applicable energy decomposition schemes available for the MR-AQCC method, while the presented energy decomposition shown below is applicable for it as well as for any other approach, including DFT. This scheme is based on total energies computed with the respective method and does not rely on any

https://doi.org/10.1021/jacsau.1c00272
JACS Au 2021, 1, 1647−1655

asymptotic expansion scheme of the interaction energy. Second, this decomposition provides essential insights by allowing us to focus on the SOMO−SOMO interaction component, which drives the pancake bonding interaction.[39,46]

The following procedure was applied for the neutral pancake-bonded dimers:[39,46]

$$E_{\text{int}}(R) = E_{\text{Total}}(R) - E_{\text{Total}}(\text{at } 10.0\text{ Å}) = -E_{\text{binding}} \tag{2}$$

where R stands for the contact distance between the monomers. The key assumption is that the two components of the interaction are approximately additive

$$E_{\text{int}} = E_{\text{SOMO-SOMO}} + E_{\text{vdW}} \tag{3}$$

The E_{vdW} term is approximated by the interaction energy of the high-spin state (triplet in this case) $E_{\text{int}}^{\text{T}}$ and taken at the same unrelaxed ground state geometry of the singlet.[46]

$$E_{\text{vdW}} \approx E_{\text{int}}^{\text{T}}(\text{at the geometry of the singlet}) \tag{4}$$

The interaction energy and its components at the equilibrium geometry of the singlet are particularly relevant and will be listed and discussed. These assumptions were justified and validated for PLY_2.[39]

The following approximation will be used for both the neutral and the charged PLY and PF−PLY dimers:

$$E_{\text{SOMO-SOMO}}(60) \approx E_{\text{int}}(60) - E_{\text{int}}(30°) \tag{5}$$

An important aspect of this approximation is that it is applicable for the singly charged PLY_2 and PF−PLY_2 dimers, while the approximation based on eqs 3 and 4 is not applicable because these are doublet ground-state dimers. As a validation, we refer to ref 39, where the rotation-based method and the multiplicity-based method gave very close estimates for the value of $E_{\text{SOMO-SOMO}}$.

The intermolecular Coulomb interaction energy (E_{Coul}) is defined by equ 6

$$E_{\text{Coul}} = \sum \frac{q_i * q_j}{d_{ij}} \tag{6}$$

where the q_i and q_j are the atomic charges and d_{ij} is the distance between the atoms i and j. The summation is limited to atom pairs that belong to different monomers in the dimer.

As an alternative, we also used the energy decomposition analysis (EDA) developed by Ziegler and Rauk,[34] using (U)PBE0-MBD[47]/TZP level of theory with the ADF[48] program package. The many-body dispersion (MBD) refers to the method of Tkatchenko et al.[47] that provides an accurate description of vdW interactions, which include both screening effects and a high-order treatment of the many-body van der Waals energy. The interaction energy and its components are denoted here differently from those in eqs 3−5, with a Δ symbol to refer specifically to the EDA analysis. ΔE_{int} is the difference between the energy of the dimer and the energies of the constituent monomers. In the current case, it is divided into four main components as follows:

$$\Delta E_{\text{int}} = \Delta E_{\text{elstat}} + \Delta E_{\text{Pauli}} + \Delta E_{\text{orb}} + \Delta E_{\text{disp}} \tag{7}$$

The term ΔE_{elstat} corresponds to the quasi-classical electrostatic interaction between the unperturbed charge distributions calculated from the orbital densities. The Pauli repulsion, ΔE_{Pauli}, contains the destabilizing interactions between electrons of the same spin on either fragment. The orbital interaction ΔE_{orb} accounts for charge transfer, delocalization, and polarization effects. The vdW interaction energy in this scheme, ΔE_{vdW}, is then approximately the sum of the dispersion interaction, electrostatic interaction, and the Pauli repulsion as follows:

$$E_{\text{vdW}} = E_{disp} + \Delta E_{\text{elstat}} + \Delta E_{\text{Pauli}} \tag{8}$$

Further computational details are summarized in Section 2 of the Supporting Information (SI).

3. RESULTS AND DISCUSSION

We present results in four subsections. First, we show strong evidence that while σ-bonded configurations are often energetically competitive with π-stacking configurations for pancake bonding with PBO = 1,[49] this is not the case with PBO = 1/2 dimers.[50] Then, evidence is provided to show that π-stacking geometries are maintained for PBO = 1/2 dimers, displaying subtle but systematic differences between positively and negatively charged dimers in correlation with the presence or absence of perfluorination, respectively. This is then put into the context of the total energy computations to show that, surprisingly, while the perfluorinated anion dimers have stronger pancake bonding with PBO = 1/2, for the parent unflourinated ones it is the cations that have the stronger pancake bonding. The interpretation, including an energy component analysis, indicates that changes in the intermolecular electrostatics play a key role in this effect.[15]

3.1. The Stability of the π-Dimer Versus the σ-Dimer

σ-Bonded configurations are often energetically competitive with π-stacking configurations, as shown, for example, by the presence of fluxional bonding in some phenalenyls[49,51] and their derivatives.[52] Therefore, we first investigate the effect of fluorine substitution and the total charge on the relative energies of the dimers of PLY and OPY, with key data summarized in Table 1;

Table 1. Relative Energies (kcal/mol) of π- and σ-Dimers of Neutral and Charged PLY_2 ($\mathbf{1_2}$) and PF−PLY_2 ($\mathbf{2_2}$) at the UM05-2X/6-311G(d) Level

	π^a	σ^b (RR1)	σ^b (RR2)	σ^b (RR3)	σ^b (RS1)	σ^b (RS2)
$\mathbf{1_2}$	0.0	−2.6	−2.9	−4.1	−1.2	−4.0
$\mathbf{2_2}$	0.0	−7.8	−7.1	−7.9	−6.4	−7.1
	π^a	$\pi(1)^c$	$\pi(2)^c$	$\pi(3)^c$	$\pi(4)^c$	$\pi(5)^c$
$\mathbf{1_2}$	0.0	8.4	5.7	6.3	-[d]	8.3
$\mathbf{1_2}^-$	0.0	3.2	3.4	4.6	4.4	3.2
$\mathbf{1_2}^+$	0.0	10.3	7.0	9.3	11.0	8.5
$\mathbf{2_2}$	0.0	8.5	5.1	5.5	-[d]	7.4
$\mathbf{2_2}^-$	0.0	12.4	8.3	9.5	12.6	10.7
$\mathbf{2_2}^+$	0.0	3.0	3.2	5.8	5.7	3.0

[a]A π-stacking dimer, D_{3d}. [b]Notation for σ-dimer configurations is from ref 50 and is illustrated in Figure S2. [c]The lower-symmetry π-stacked structures are illustrated in Figure S3. [d]Converges to π(3); for details, see Tables S5 and S6.

the structures are illustrated in Figure S2. We obtained results consistent with previous work[49,50] for neutral PLY_2. Among the five σ- and one π-dimer configurations for neutral PLY_2, the π-dimers are by 1.2 to 4.1 kcal/mol less stable than the σ-dimers, while the σ-dimers are more stable by 6.4 to 7.9 kcal/mol for neutral PF−PLY_2. The relative stability is reversed for each of the charged species, with the π-stacking configuration becoming more stable. Note that σ-bonding in a phenalenyl dimer is relatively weak compared to ordinary C−C σ-bonds due to the reduced π-conjugation and the stress induced by pyramidalization in an approximately planar framework.[49,50]

The corresponding charged species present a totally different picture. Since these species have a formal PBO = 1/2, one expects the σ-bonds to be much weaker since only one unpaired electron is available. Indeed, during the geometry optimization process aimed at obtaining σ-dimers, we started from the optimized geometries of the various neutral σ-dimers; however, all these optimizations converged to various π-dimers with novel

https://doi.org/10.1021/jacsau.1c00272
JACS Au 2021, 1, 1647−1655

Table 2. Intermolecular Carbon−Carbon Distances (Å) of the Neutral and Charged PLY (1), PF−PLY (2), OPY (3), and PF-OPY (4) π-Stacking Pancake-Bonded Dimers[a]

	bond order, PBO	D_{cc} ($D_{0,0}$)	$D_{\alpha\alpha}$ ($D_{3,3}$)	$D_{2,4}$	$D_{1,5}$	average[d]
$\mathbf{1}_2$	1	3.061	2.991			3.001
$\mathbf{1}_2^+$	1/2	3.187	3.191			3.190
$\mathbf{1}_2^-$	1/2	3.248	3.210			3.215
$\mathbf{2}_2$	1	3.099	2.981			2.998
$\mathbf{2}_2^+$	1/2	3.166	3.052			3.068
$\mathbf{2}_2^-$	1/2	3.120	3.016			3.031
$\mathbf{3}_2$	1	3.186	3.148	3.175	3.161	3.169
$\mathbf{3}_2^+$	1/2	3.202	3.246	3.234	3.188	3.221
$\mathbf{3}_2^-$	1/2	3.274	3.233	3.245	3.250	3.249
$\mathbf{4}_2$	1	3.164	3.015	3.049	3.097	3.075
$\mathbf{4}_2^+$	1/2	3.185	3.052	3.069	3.118	3.099
$\mathbf{4}_2^-$	1/2	3.171	3.028	3.059	3.107	3.085
$\mathbf{1}_2$ (Exp.[b])	1	3.109 (3.201)	3.176 (3.306)			3.188 (3.291)
$\mathbf{3}_2$ (Exp.[c])	1	3.216 (3.257)	3.203 (3.256)	3.205/3.210 (3.180/3.327)	3.182 (3.225)	3.200 (3.247)

[a]All geometries refer to optimized structures by (U)M05-2X/6-311G(d). All neural and charged dimers of **1** and **2** have D_{3d} symmetry, and all neutral and charged dimers of **3** and **4** have C_{2h} symmetry. Atomic numbering corresponds to Scheme 1. Exp. indicates the inclusion of bulky side groups in the computation and the respective experimental value is in parentheses. [b]Ref 20. [c]Ref 21. [d]Average direct $C_\alpha \cdots C_\alpha$ contact distances.

unique structures, each of which displayed local minima with only one or two close contacts between the α-carbon atoms. Most importantly, during the geometry optimization we were unable to find any local minima corresponding to a σ-dimer. Note that all these additionally identified π-dimers (listed in Table 1 and illustrated in Figure S3) are less stable and in most cases significantly less stable than the staggered D_{3d} π-dimer configuration. This indicates that the multicenter pancake bonding shows strong preference for the maximum of the SOMO−SOMO overlapping geometry even with one or three electrons (1e/mc or 3e/mc). We will gain further insights into this effect based on the geometry and energy analysis in the next sections.

The relative weakness of the σ-bonded configuration for the singly charged PLY_2 can be understood as follows. First, the σ-bond is much weaker for a single or three electron bond versus a two-electron bond. Second, the local pyramidalization needed for σ-bond formation distorts the rigid plane of the π-conjugated monomer and disrupts the conjugation, also disfavoring the σ-dimer configuration compared to the π-dimer configuration. Third, shorter intermolecular distances in the σ-dimer increase the Coulomb repulsion compared to that in the π-dimer. These effects make the π-dimer configuration more favorable compared to the σ-dimer, so much so that σ-dimers do not even exist as local minima for the charged PLY_2 and PF−PLY_2 dimers. It appears that many pancake-bonded molecular dimers and larger aggregates avoid σ-bonding due to these effects.[31,32,53,54]

3.2. The Effect of Charge on the Structures of the π-Dimers

The most remarkable charge effect can be seen when comparing the direct C−C intermolecular distances in the geometries of the 12 optimized π-dimers, four neutral ones with full PBO = 1 and eight charged ones with PBO = 1/2, which are given in Table 2 and Table S7. Note that the geometry optimization at the MR-AQCC/6-31G(d) level for the PLY systems shown in Table S7 displays the same trends as the DFT geometry data shown in Table 2. The surprising overall observation is that all these contact distances are without exception significantly shorter than 3.40 Å, the vdW distance for C⋯C contacts. Due to the SOMO orbital, both PLY^+ and PLY^- are stable, making the preparation of these charged dimer species viable. The cationic PLY_2^+ has clearly shorter average intermolecular distances as compared to those of the anionic species, PLY_2^-, while both correspond to PBO = 1/2. The situation is reversed for the perfluorinated species, where PF−PLY_2^+ has significantly longer intermolecular distances as compared to those of the anionic species, PF−PLY_2^-. Similar trends are seen in the charged dimers of OPY and PF-OPY. This is quite significant because it implies a control over contact distances and thereby allows a control of bandwidths in pancake-bonded systems not seen before.

3.3. Energetics of the π-Dimers

The interaction energy values are collected in Table 3 for all 12 dimeric species discussed in this work. Table S9 provides validation results at a higher optimization level for the six smaller systems.

Table 3. Intermolecular Interaction Energies and Their $E_{SOMO-SOMO}$ Components of the Neutral and Charged PLY (1), PF−PLY (2), OPY (3), and PF-OPY (4) Dimers Obtained by MR-AQCC/6-31G(d)//UM05-2X/6-311G(d)

	$\mathbf{1}_2$	$\mathbf{1}_2^+$	$\mathbf{1}_2^-$	$\mathbf{2}_2$	$\mathbf{2}_2^+$	$\mathbf{2}_2^-$
E_{int}	−10.8	−19.6	−11.3	−16.7	−16.9	−25.7
$E_{SOMO-SOMO}$	−22.3	−15.1	−12.0	−13.9	−13.3	−11.7
E_{vdW}	11.5	−4.5	0.7	−2.8	−3.6	−14.0
	$\mathbf{3}_2$	$\mathbf{3}_2^+$	$\mathbf{3}_2^-$	$\mathbf{4}_2$	$\mathbf{4}_2^+$	$\mathbf{4}_2^-$
E_{int}	−10.9	−21.8	−12.9	−15.7	−20.0	−28.3
$E_{SOMO-SOMO}$	−14.1	–[a]	–[a]	−10.3	–[a]	–[a]
E_{vdW}	3.1	–[a]	–[a]	−5.4	–[a]	–[a]

[a]Data not available, see text below eq 5.

The most prominent result is that the largest binding energy (the most negative interaction energy) was obtained not for the dimers with PBO = 1 but for specific charged dimers with the bond order of only PBO = 1/2. This unusual effect was first observed for $\mathbf{1}_2^+$ and was attributed to electrostatic effects.[50] Here we find that the effect extends to $\mathbf{3}_2^+$, $\mathbf{2}_2^-$, and $\mathbf{4}_2^-$. This complex behavior, especially the dependence on the sign of the charge on the dimer, needs interpretation; the binding energy is larger for positively charged dimers of PLY and OPY and larger

https://doi.org/10.1021/jacsau.1c00272
JACS Au 2021, 1, 1647−1655

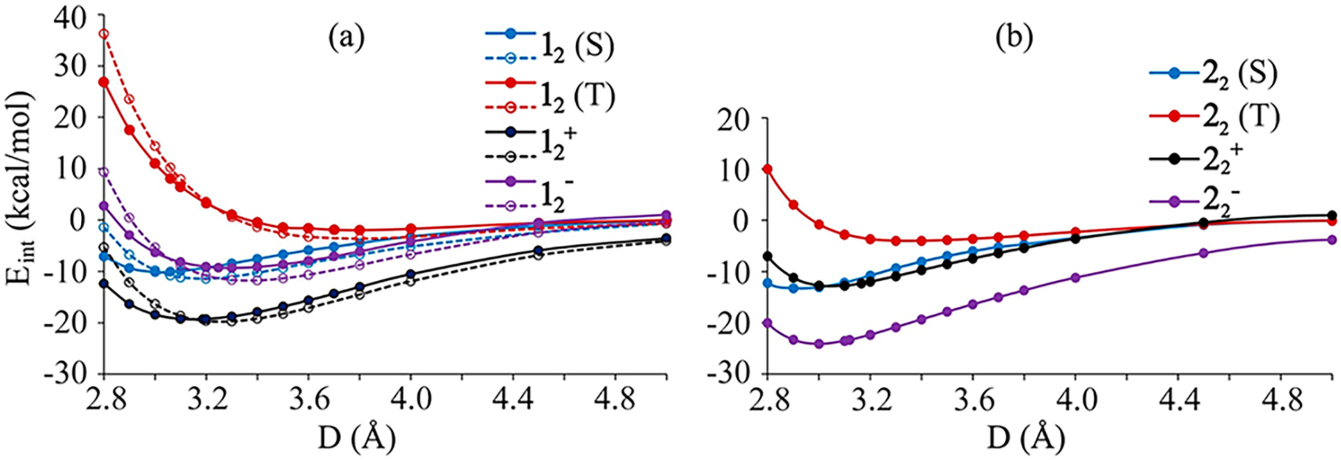

Figure 1. (a) Rigid dissociation energy scans of singlet and triplet states of the phenalenyl dimer (**1**$_2$, PLY_2) and the doublet states of the charged phenalenyl dimers (PLY_2^+ and PLY_2^-) in the D_{3d} staggered configuration as a function of the intermolecular distance (D_{cc}) using MR-AQCC(n, 2)/3-21G, where the values of n = 1−3 correspond to the cationic, neutral, and anionic dimers, respectively. (b) The scans of the neutral and the charged PF−PLY dimers (**2**$_2$). In panel a, the dashed line corresponds to the MR-AQCC(n, 2)/6-31G(d) level.

for the negatively charged dimers of the perfluorinated species PF−PLY and PF-OPY. The differences are dramatic considering the scale of the typical intermolecular interactions, adding approximately 9−13 kcal/mol to the binding energies for **1**$_2^+$, **2**$_2^-$, **3**$_2^+$, and **4**$_2^-$ compared to those of their neutral counterparts according to Table 2. In what follows, we trace the enhancement of the interaction to electrostatic effects.

The total energy scans provide further insights. Figure 1 shows energy scans with respect to the intermolecular distance, D_{cc}, for the all six PLY dimers plus the triplets of the two neutral ones. Note that the 3-21G basis set presents a good performance with reference to 6-31G(d) (Figure 1a, dashed line) using the MR-AQCC method. The significant electrostatic interaction accounts for the lowest E_{int} value in the cationic PLY_2^+ and anionic PF−PLY_2^- dimers, which will be discussed in the next subsection.

Most striking is the fact that even at long range, where overlap is nearly negligible, a clearly enhanced interaction appears for PLY_2^+ compared to both PLY_2 and PLY_2^-, while for the perfluoro case the opposite charge is preferred, as PF−PLY_2^- is more stable near dissociation compared to PF−PLY_2 and PLY_2^+. This behavior provides further evidence that the preference is directed by the electrostatic interaction in the distance range relevant for pancake bonding. At distances shorter than the equilibrium distances for the dimers, the orders of some of these states interchange, as shown in Figure 1.

Next, we analyze the interaction energy by reporting rotational scans based on the M05-2X/6-311G(d) geometries and using the energy at the MR-AQCC/6-31G(d) level. The respective E_{vdW} and $E_{SOMO-SOMO}$ terms for all six PLY-based dimers are listed in Table 3. While the approximations presented in eqs 3 and 4 do not separate out the electrostatic component from the dispersion attraction and Pauli repulsion components, we can discuss the rest of the trends as follows. For PLY_2, the total vdW term is positive and contains some Pauli repulsion due to the shorter-than-vdW contacts. The negative charge distributed in the intermolecular space in the neutral dimer provides another repulsive term. The latter is reduced in the positively charged PLY_2^+ compared to the negatively charged PLY_2^-. The elongated C···C contacts in the charged dimers mentioned in connection with Table 2 reduce the Pauli repulsion. Assuming that changes in the dispersion energy are less sensitive to the single charge added to the dimer, this explains that the total vdW interaction becomes a negative (attractive) value for PLY_2^+ and becomes less repulsive for PLY_2^- as compared to the neutral PLY_2 dimer. For the PF−PLY_2 series, the effects of the signs of the charges are reversed, as discussed above.

For the PLY_2 dimer, the $E_{SOMO-SOMO}$ term is significantly lower in the charged species as compared to that for the neutral one, but the vdW repulsion that includes the reduced electrostatic repulsion even becomes attractive in the cationic dimer. Thus, the largest binding energy occurs for the cationic dimer despite the reduced $E_{SOMO-SOMO}$ value. The $E_{SOMO-SOMO}$ terms all are smaller in the PF−PLY_2 series as compared to those in the PLY_2 series, but the vdW interaction becomes attractive for PF−PLY_2^+. The anionic PF−PLY_2^- dimer has a large attractive vdW interaction, leading to the largest binding energy in the PF−PLY series. The reduction of the SOMO−SOMO interaction in the PLY_2 series upon charging affects the overall properties of pancake-bonded systems because this reduction amounts to a reduction of the strong preference for specific orientations for pancake-bonded systems. Nevertheless, as demonstrated by the data in Figure S1(c) and Table 3, the SOMO−SOMO energy term leads to a barrier of 12 to 22 kcal/mol between the low- and high-energy conformers, a sufficiently large driving force to strongly favor one of the two atom-over-atom configurations, which in the case of all PLY dimers discussed is the D_{3d} staggered configuration.

3.4. Consequences of the Electrostatic Environment

In this subsection, we trace the following trends based on the computed total interaction energies shown in Table 3 to differences in intermolecular electrostatic interactions in the dimers under study.

These trends are as follows:

1. For the unflourinated dimers, the absolute values of the interaction energies are larger by 8−9 kcal/mol for the positively charged dimers: **1**$_2^+$ vs **1**$_2^-$ and **3**$_2^+$ vs **3**$_2^-$.
2. For the perfluorinated dimers, the absolute values of the interaction energies are larger by 8−9 kcal/mol for the negatively charged dimers: **2**$_2^-$ vs **2**$_2^+$ and **4**$_2^-$ vs **4**$_2^+$.

The same trends are reflected in the average optimized contact distances (in Table 1) that are slightly shorter for the

https://doi.org/10.1021/jacsau.1c00272
JACS Au 2021, 1, 1647−1655

positively charged unflourinated dimers and the *negatively* charged perfluorinated dimers.

We employ qualitative arguments, followed by two approaches toward energy decomposition: Coulomb interaction energies based on the atomic point charge model and a Morokuma−Ziegler−Rauk-type EDA.[33,34,55,56] It is worth mentioning that energy decomposition is only able to provide trends, since the interaction energy component terms are not physical observables.[57]

These trends in the C···C contact distances can be qualitatively understood on the basis of the charge distributions around the monomers as illustrated in Scheme 3, which

Scheme 3. NPA Charge Distribution in |e| (Top Row) and Electrostatic Potential (ESP) (Bottom Row; kcal/mol) Mapped on the van der Waals Surface (ρ = 0.001 a.u. Isosurface) of the Neutral Unsubstituted PLY (1) and OPY (3) and the Perfluoro-Substituted PF−PLY (2) and PF−OPY (4)[a]

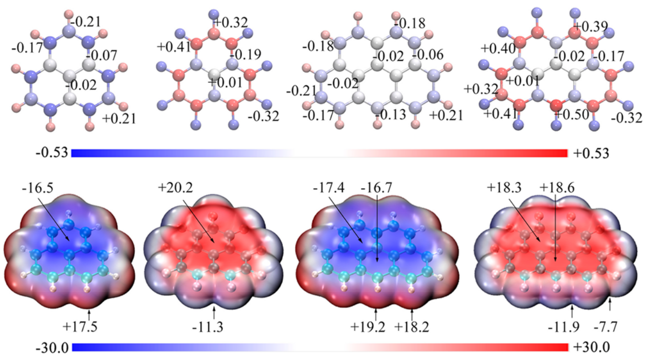

1 2 3 4

[a]Computed by UM05-2X/6-311G(d).

highlights that the charge distributions and electrostatic potentials have opposite signs between unflourinated and perfluorinated monomers. The strongly polarized distribution of the atomic charges in PLY$^-$ and PF−PLY$^+$ is at the source of their relatively longer contacts compared to those of the oppositely charged PLY$^+$ and PF−PLY$^-$. Based on the charge distribution in Schemes 3 and S2 (charged species), the efficient way to reduce the intermolecular electrostatic repulsion would require an extra positive charge for PLY and OPY and an extra negative charge on PF−PLY and PF-OPY.

We follow these arguments with Coulomb interaction energies based on point charges, as summarized in Tables 4 and S8a and b. Atomic charges, as is well-known, can differ strongly. However, the atomic point charge-based intermolecular Coulomb interaction is well-defined by eq 6.

These data support the qualitative conclusions based on the charge distributions of the monomers discussed above in connection with Scheme 3. The singlet and triplet Coulomb interaction energy terms of the neutral dimers are virtually the same for all four systems, which is in line with eq 4. More importantly, comparing the positively charged nonfluorinated $\mathbf{1}_2^+$ and $\mathbf{3}_2^+$ to the negatively charged $\mathbf{1}_2^-$ and $\mathbf{3}_2^-$, the latter are strongly destabilized by approximately 23−25 kcal/mol. This substantial effect is the source of the relative preference for the positively charged dimers versus the negatively charged dimers. For the perfluorinated dimers, the charge preference has the opposite sign; in this case the negatively charged dimers display an approximately 33 kcal/mol preference over the positively

Table 4. Intermolecular Coulomb Interaction Energy (E_{Coul}; kcal/mol) of Dimers Based on Atomic Point Charges from Natural Population Analysis (NPA) by UM05-2X/6-311G(d)[a]

	$\mathbf{1}_2$[b]	$\mathbf{1}_2^+$	$\mathbf{1}_2^-$	$\mathbf{1}_2$[c]
E_{Coul}	15.9	19.2	42.4	15.6
	$\mathbf{2}_2$[b]	$\mathbf{2}_2^+$	$\mathbf{2}_2^-$	$\mathbf{2}_2$[c]
E_{Coul}	31.8	63.8	31.0	31.8
	$\mathbf{3}_2$[b]	$\mathbf{3}_2^+$	$\mathbf{3}_2^-$	$\mathbf{3}_2$[c]
E_{Coul}	18.1	19.7	45.0	17.9
	$\mathbf{4}_2$[b]	$\mathbf{4}_2^+$	$\mathbf{4}_2^-$	$\mathbf{4}_2$[c]
E_{Coul}	35.9	67.3	34.0	35.9

[a]All geometries correspond to the optimized structures, except for the triplet that corresponds to the geometry of the optimized singlet. [b]Singlet. [c]Triplet.

charged ones when considering these point charge-based models for estimating the Coulomb repulsion. Due to their intrinsically arbitrary elements, these models are not conclusive but do support the switch of preference between the positively and negatively charged dimers as a function of the perfluorination.

The alternative to a point charge model for estimating intermolecular electrostatic interactions is the use of quantum mechanical energy decomposition schemes. While such schemes are plagued by various limitations,[57,58] for the current purposes they still provide useful insights into the origin of the charge effects under discussion. The respective data are presented in Table 5 and Figure S4.

Table 5. Energy Decomposition Analysis (EDA; kcal/mol) of the Intermolecular Interaction Energy in the Neutral and Charged Dimers of PLY (1), PF−PLY (2), OPY (3), and PF-OPY (4) using UPBE0-MBD/TZP//UM05-2X/6-311G(d) at the Most Stable D_{3d} and C_{2h} Configurations[a]

	$\mathbf{1}_2$	$\mathbf{1}_2^+$	$\mathbf{1}_2^-$	$\mathbf{2}_2$	$\mathbf{2}_2^+$	$\mathbf{2}_2^-$
ΔE_{int}	−12.9	−24.5	−15.6	−12.7	−18.2	−26.9
$\Delta E_{\mathrm{Pauli}}$	47.6	26.4	27.3	38.6	30.4	37.8
$\Delta E_{\mathrm{elstat}}$	−22.2	−16.2	−8.3	−15.2	−4.7	−23.0
ΔE_{disp}	−14.9	−12.6	−13.1	−18.3	−17.3	−18.1
ΔE_{orb}	−23.4	−22.2	−21.4	−17.8	−26.7	−23.7
	$\mathbf{3}_2$	$\mathbf{3}_2^+$	$\mathbf{3}_2^-$	$\mathbf{4}_2$	$\mathbf{4}_2^+$	$\mathbf{4}_2^-$
ΔE_{int}	−15.4	−28.3	−18.6	−18.0	−22.2	−30.7
$\Delta E_{\mathrm{Pauli}}$	40.8	35.0	34.0	44.7	40.8	45.7
$\Delta E_{\mathrm{elstat}}$	−19.2	−21.2	−11.9	−17.8	−9.0	−26.2
ΔE_{disp}	−20.7	−19.5	−20.0	−26.3	−25.6	−26.4
ΔE_{orb}	−16.3	−22.6	−20.7	−18.7	−28.4	−23.8

[a]The terms refer to equ 7.

The key result of this analysis is as follows. The electrostatic energy, $\Delta E_{\mathrm{elstat}}$, provides a relative preference of −8 to −10 kcal/mol for $\mathbf{1}_2^+$ and $\mathbf{3}_2^+$ compared to $\mathbf{1}_2^-$ and $\mathbf{3}_2^-$, respectively. For the perfluorinated pairs, this additional electrostatic stabilization was computed at −17 to −18 kcal/mol. While the specific decomposition depends on the details of the level of theory and the overlap between the interacting molecules, there should be no doubt about the importance of the electrostatic component of the intermolecular interaction to explain the relative stabilities of these pancake-bonded dimers as a function of charge *and* perfluorination.

https://doi.org/10.1021/jacsau.1c00272
JACS Au 2021, 1, 1647−1655

A brief overview of the other terms of this EDA shows consistency with respect to the analysis based on eqs 3 and 4. The orbital interaction term, ΔE_{orb}, accounts for the charge transfer, delocalization, and polarization effects, which can also be considered to include the main contributions to the SOMO−SOMO interaction, while the other three terms (ΔE_{elstat}, ΔE_{Pauli}, and ΔE_{disp}) added together can be considered to represent the vdW interaction, ΔE_{vdW}, as used in eq 3 above. Figure S4a and b show the total energy curves of the four main components of the EDA as a function of θ for PLY_2 and $PF-PLY_2$, respectively. Figure S4c displays the difference between singlet and triplet scans, which approximately represents the SOMO−SOMO interaction as per eqs 3 and 4. Compared to that for the PLY_2 dimer, the magnitude of the SOMO−SOMO interaction is significantly smaller in the $PF-PLY_2$ dimer, which is fully consistent with our MR-AQCC analysis. Moreover, it reflects that the SOMO−SOMO interaction is the main component for the difference of the total interaction between the singlet and the triplet. On the other hand, ΔE_{elstat} and ΔE_{disp} are nearly constant, and the value of ΔE_{Pauli} has only small variations, indicating that ΔE_{vdW} does not change significantly from 60° to 30°, which is again consistent with our MR-AQCC analysis.

For the neutral dimers in their singlet states, the orbital term is smaller in $PF-PLY_2$ as compared to that in PLY_2; however, the former has a larger dispersion term, which is consistent with the rotational scans. Comparing the different-charged PLY_2 or $PF-PLY_2$ dimers, the electrostatic term is a crucial factor in strengthening the interaction, as reflected in ΔE_{int}. This provides further evidence that the PLY_2^+ and $PF-PLY_2^-$ have stronger overall pancake bonds compared to the oppositely charged dimers, PLY_2^- and $PF-PLY_2^+$, respectively.

Additional supporting evidence for this interpretation is provided by data in Table S10, which displays the total number of effectively unpaired electrons for all 12 dimers under discussion. This parameter signals a degree of electron unpairing on a comparable scale across each of the two series. These data confirm the trends, showing that electron pairing decreases (N_U increases) upon the charged dimers moving from PBO = 1 to 1/2 as expected, further underlining the point that the strength of pancake bonding for this charge effect is not due to increased electron pairing but instead to a reduced electrostatic repulsion between the PAHs.

4. CONCLUSION

As a practical matter, properly charged pancake-bonded systems can increase their stability and avoid σ-bonding more easily than neutral pancake-bonded systems. The second observation is that the charged dimers can display stronger pancake bonding compared to the neutral radical-based dimers even though charging reduces the formal pancake bond order from 1 to 1/2. The associated intermolecular distances with PBO = 1/2 are typically longer than those of pancake bonds with PBO = 1.

The interaction energy in charged pancake-bonded systems is less dominated by the SOMO−SOMO interactions, and electrostatic effects become more important. The reduced SOMO−SOMO interaction in the PLY_2 and OPY_2 series upon charging is still sufficiently robust to maintain their strong preferences for the specific orientations typical for pancake-bonded systems by maintaining a maximum overlap with atom-over-atom configurations.

■ ASSOCIATED CONTENT

Supporting Information

The Supporting Information is available free of charge at https://pubs.acs.org/doi/10.1021/jacsau.1c00272.

Atomic notation, SOMO coefficients, computational details, energy scans, structures and coordinates of dimers, energy decomposition, Coulomb energies, charge distribution, and physical properties (PDF)

■ AUTHOR INFORMATION

Corresponding Authors

Zhong-hua Cui − *Institute of Atomic and Molecular Physics, Key Laboratory of Physics and Technology for Advanced Batteries (Ministry of Education), Jilin University, Changchun 130012, P. R. China; Beijing National Laboratory for Molecular Sciences, Beijing 100190, P. R. China;* orcid.org/0000-0002-0710-1774; Email: zcui@jlu.edu.cn

Miklos Kertesz − *Chemistry Department and Institute of Soft Matter, Georgetown University, Washington, D.C 20057-1227, United States;* orcid.org/0000-0002-7930-3260; Email: kertesz@georgetown.edu

Authors

Meng-hui Wang − *Institute of Atomic and Molecular Physics, Key Laboratory of Physics and Technology for Advanced Batteries (Ministry of Education), Jilin University, Changchun 130012, P. R. China*

Hans Lischka − *Department of Chemistry and Biochemistry, Texas Tech University, Lubbock, Texas 79409, United States; A School of Pharmaceutical Science and Technology, Tianjin University, Tianjin 300072, P. R. China;* orcid.org/0000-0002-5656-3975

Complete contact information is available at: https://pubs.acs.org/10.1021/jacsau.1c00272

Notes

The authors declare no competing financial interest.

■ ACKNOWLEDGMENTS

This work was funded by the National Natural Science Foundation of China (nos 11874178, 11922405, and 91961204). This work was supported by Beijing National Laboratory for Molecular Sciences (BNLMS201910). M.K. is member of the Georgetown University Institute of Soft Matter. Computer time was partially provided by the School of Pharmaceutical Science and Technology, Tianjin University on the computer cluster Arran, which is gratefully acknowledged.

■ REFERENCES

(1) Schafer, D. E.; Wudl, F.; Thomas, G. A.; Ferraris, J. P.; Cowan, D. O. Apparent Giant Conductivity Peaks in an Anisotropic Medium: TTF-TCNQ. *Solid State Commun.* **1974**, *14*, 347−351.

(2) Soos, Z. G.; Klein, D. J. Charge-Transfer in Solid State Complexes. In *Molecular Association*, Vol. *1*; Foster, R., Ed.; Academic Press: New York, NY, 1975.).

(3) Heeger, A. J. Charge-Density Wave Phenomena in One-Dimensional Metals: TTF-TCNQ and Related Organic Conductors. In *Highly Conducting One-Dimensional Solids*; Devreese, J., Ed.; Springer: Boston, MA, 1979; pp 69−145.

(4) Miller, J. *Extended Linear Chain Compounds*, Vols *1*−*3*; Springer: New York, NY, 1982.

https://doi.org/10.1021/jacsau.1c00272
JACS Au 2021, 1, 1647−1655

(5) Pal, S. K.; Itkis, M. E.; Tham, F. S.; Reed, R. W.; Oakley, R. T.; Haddon, R. C. Resonating valence-bond ground state in a phenalenyl-based neutral radical conductor. *Science* **2005**, *309*, 281−284.

(6) Chen, P. C.; Metz, J. N.; Mennito, A. S.; Merchant, S.; Smith, S. E.; Siskin, M.; Rucker, S. P.; Dankworth, D. C.; Kushnerick, J. D.; Yao, N.; Zhang, Y. L. Petroleum pitch: Exploring a 50-year structure puzzle with real-space molecular imaging. *Carbon* **2020**, *161*, 456−465.

(7) Geraskina, M. R.; Dutton, A. S.; Juetten, M. J.; Wood, S. A.; Winter, A. H. The Viologen Cation Radical Pimer: A Case of Dispersion-Driven Bonding. *Angew. Chem., Int. Ed.* **2017**, *56*, 9435−9439.

(8) Penneau, J. F.; Stallman, B. J.; Kasai, P. H.; Miller, L. L. An Imide Anion Radical That Dimerizes and Assembles into. Pi.-Stacks in Solution. *Chem. Mater.* **1991**, *3*, 791−796.

(9) Kosower, E. M.; Cotter, J. L. Stable Free Radicals. II. The Reduction of 1-Methyl-4-cyanopyridinium Ion to Methylviologen Cation Radical. *J. Am. Chem. Soc.* **1964**, *86*, 5524−5527.

(10) Tian, Y. H.; Kertesz, M. Is There a Lower Limit to the CC Bonding Distances in Neutral Radical pi-Dimers? The Case of Phenalenyl Derivatives. *J. Am. Chem. Soc.* **2010**, *132*, 10648−10649.

(11) Haddon, R. C. Design of Organic Metals and Superconductors. *Nature* **1975**, *256*, 394−396.

(12) Kertesz, M. Pancake Bonding: An Unusual Pi-Stacking Interaction. *Chem. - Eur. J.* **2019**, *25*, 400−416.

(13) Preuss, K. E. Metal-radical coordination complexes of thiazyl and selenazyl ligands. *Coord. Chem. Rev.* **2015**, *289*, 49−61.

(14) Devic, T.; Yuan, M.; Adams, J.; Fredrickson, D. C.; Lee, S.; Venkataraman, D. The maximin principle of pi-radical packings. *J. Am. Chem. Soc.* **2005**, *127*, 14616−14627.

(15) Small, D.; Zaitsev, V.; Jung, Y. S.; Rosokha, S. V.; Head-Gordon, M.; Kochi, J. K. Intermolecular, pi-to-pi bonding between stacked aromatic dyads. Experimental and theoretical binding energies and near-IR optical transitions for phenalenyl radical/radical versus radical/cation dimerizations. *J. Am. Chem. Soc.* **2004**, *126*, 13850−13858.

(16) Jung, Y. S.; Head-Gordon, M. What is the nature of the long bond in the $TCNE_2^{2-}$ pi-dimer? *Phys. Chem. Chem. Phys.* **2004**, *6*, 2008−2011.

(17) Lu, J. M.; Rosokha, S. V.; Kochi, J. K. Stable (long-bonded) dimers via the quantitative self-association of different cationic, anionic, and uncharged pi-radicals: Structures, energetics, and optical transitions. *J. Am. Chem. Soc.* **2003**, *125*, 12161−12171.

(18) Jakowski, J.; Simons, J. Analysis of the electronic structure and bonding stability of the TCNE dimer dianion $(TCNE)_2^{2-}$. *J. Am. Chem. Soc.* **2003**, *125*, 16089−16096.

(19) Novoa, J. J.; Lafuente, P.; Del Sesto, R. E.; Miller, J. S. Exceptionally long (> = 2.9 angstrom) C-C bonds between $[TCNE]^-$ ions: Two-electron, four-center pi*-pi* C-C bonding in pi-$[TCNE]_2^{2-}$. *Angew. Chem., Int. Ed.* **2001**, *40*, 2540−2545.

(20) Goto, K.; Kubo, T.; Yamamoto, K.; Nakasuji, K.; Sato, K.; Shiomi, D.; Takui, T.; Kubota, M.; Kobayashi, T.; Yakusi, K.; Ouyang, J. Y. A stable neutral hydrocarbon radical: Synthesis, crystal structure, and physical properties of 2,5,8-tri-tert-butyl-phenalenyl. *J. Am. Chem. Soc.* **1999**, *121*, 1619−1620.

(21) Xiang, Q.; Guo, J.; Xu, J.; Ding, S. S.; Li, Z. Y.; Li, G. W.; Phan, O. A.; Gu, Y. W.; Dang, Y. F.; Xu, Z. Q.; Gong, Z. C.; Hu, W. P.; Zeng, Z. B.; Wu, J. S.; Sun, Z. Stable Olympicenyl Radicals and Their pi-Dimers. *J. Am. Chem. Soc.* **2020**, *142*, 11022−11031.

(22) Miller, J. S.; Novoa, J. J. Four-center carbon-carbon bonding. *Acc. Chem. Res.* **2007**, *40*, 189−196.

(23) Roach, A. C.; Baybutt, P. Potential curves of alkali diatomic molecules and the origins of bonding anomalies. *Chem. Phys. Lett.* **1970**, *7*, 7−10.

(24) Hofmann, P. E.; Tripp, M. W.; Bischof, D.; Grell, Y.; Schiller, A. L. C.; Breuer, T.; Ivlev, S. I.; Witte, G.; Koert, U. Unilaterally Fluorinated Acenes: Synthesis and Solid-State Properties. *Angew. Chem., Int. Ed.* **2020**, *59*, 16501−16505.

(25) Meot-Ner, M. Dimer cations of polycyclic aromatics. Experimental bonding energies and resonance stabilization. *J. Phys. Chem.* **1980**, *84*, 2724−2728.

(26) Badger, B.; Brocklehurst, B. Formation of Dimer Cations of Aromatic Hydrocarbons. *Nature* **1968**, *219*, 263−263.

(27) Howarth, O. W.; Fraenkel, G. K. Electron Spin Resonance Study of Mono- and Dimeric Cations of Aromatic Hydrocarbons1. *J. Am. Chem. Soc.* **1966**, *88*, 4514−4515.

(28) Suzuki, S.; Morita, Y.; Fukui, K.; Sato, K.; Shiomi, D.; Takui, T.; Nakasuji, K. Aromaticity on the pancake-bonded dimer of neutral phenalenyl radical as studied by MS and NMR spectroscopies and NICS analysis. *J. Am. Chem. Soc.* **2006**, *128*, 2530−2531.

(29) Bogdanov, N. E.; Milašinović, V.; Zakharov, B. A.; Boldyreva, E. V.; Molcanov, K. Pancake-bonding of semiquinone radicals under variable temperature and pressure conditions. *Acta Crystallogr., Sect. B: Struct. Sci., Cryst. Eng. Mater.* **2020**, *76*, 285−291.

(30) Starodub, T. N.; Cizmar, E.; Kliuikov, A.; Starodub, V. A.; Feher, A.; Kozlowska, M. Stabilization of Pancake Bonding in $(TCNQ)^2$ (center dot-) Dimers in the Radical-Anionic Salt (N-CH_3-2-NH_2-5Cl-Py)(TCNQ)(CH_3CN) Solvate and Antiferromagnetism Induction. *ChemistryOpen* **2019**, *8*, 984−988.

(31) Molcanov, K.; Jelsch, C.; Landeros, B.; Hernandez-Trujillo, J.; Wenger, E.; Stilinovic, V.; Kojic-Prodic, B.; Escudero-Adan, E. C. Partially Covalent Two-Electron/Multicentric Bonding between Semiquinone Radicals. *Cryst. Growth Des.* **2019**, *19*, 391−402.

(32) Molcanov, K.; Stalke, D.; Santic, A.; Demeshko, S.; Stilinovic, V.; Mou, Z. Y.; Kertesz, M.; Kojic-Prodic, B. Probing semiconductivity in crystals of stable semiquinone radicals: organic salts of 5,6-dichloro-2,3-dicyanosemiquinone (DDQ) radical anions. *CrystEngComm* **2018**, *20*, 1862−1873.

(33) Morokuma, K. Why Do Molecules Interact? The Origin of Electron Donor-Acceptor Complexes, Hydrogen Bonding and Proton Affinity. *Acc. Chem. Res.* **1977**, *10*, 294−300.

(34) Ziegler, T.; Rauk, A. On the Calculation of Bonding Energies by the Hartree Fock Slater Method. *Theor. Chim. Acta.* **1977**, *46*, 1−10.

(35) Szalay, P. G.; Bartlett, R. J. Multi-Reference Averaged Quadratic Coupled-Cluster Method: A Size-Extensive Modification of Multi-Reference CI. *Chem. Phys. Lett.* **1993**, *214*, 481−488.

(36) Szalay, P. G.; Muller, T.; Gidofalvi, G.; Lischka, H.; Shepard, R. Multiconfiguration Self-Consistent Field and Multireference Configuration Interaction Methods and Applications. *Chem. Rev.* **2012**, *112*, 108−181.

(37) Lischka, H.; Shepard, R.; Muller, T.; Szalay, P. G.; Pitzer, R. M.; Aquino, A. J. A.; Araújo do Nascimento, M. M. A.; Barbatti, M.; Belcher, L. T.; Blaudeau, J. P.; Borges, I.; Brozell, S. R.; Carter, E. A.; Das, A.; Gidofalvi, G.; Gonzalez, L.; Hase, W. L.; Kedziora, G.; Kertesz, M.; Kossoski, F.; Machado, F. B. C.; Matsika, S.; do Monte, S. A.; Nachtigallova, D.; Nieman, R.; Oppel, M.; Parish, C. A.; Plasser, F.; Spada, R. F. K.; Stahlberg, E. A.; Ventura, E.; Yarkony, D. R.; Zhang, Z. Y. The generality of the GUGA MRCI approach in COLUMBUS for treating complex quantum chemistry. *J. Chem. Phys.* **2020**, *152*, 134110.

(38) Zhao, Y.; Schultz, N. E.; Truhlar, D. G. Design of density functionals by combining the method of constraint satisfaction with parametrization for thermochemistry, thermochemical kinetics, and noncovalent interactions. *J. Chem. Theory Comput.* **2006**, *2*, 364−382.

(39) Cui, Z. H.; Lischka, H.; Beneberu, H. Z.; Kertesz, M. Rotational Barrier in Phenalenyl Neutral Radical Dimer: Separating Pancake and van der Waals Interactions. *J. Am. Chem. Soc.* **2014**, *136*, 5539−5542.

(40) Lischka, H.; Muller, T.; Szalay, P. G.; Shavitt, I.; Pitzer, R. M.; Shepard, R. COLUMBUS-a program system for advanced multi-reference theory calculations. *Wiley Interdiscip. Rev.: Comput. Mol. Sci.* **2011**, *1*, 191−199.

(41) Lischka, H.; Shepard, R.; Shavitt, I.; Pitzer, R. M.; Dallos, M.; Mueller, T.; Szalay, P. G.; Brown, F. B.; Ahlrichs, R.; Boehm, J. G.; Chang, A.; Comeau, D. C.; Gdanitz, R.; Dachsel, H.; Ehrhardt, C.; Ernzerhof, M.; Hoechtl, P.; Irle, S.; Kedziora, G.; Kovar, T.; Parasuk, V.; Pepper, M. J. M.; Scharf, P.; Schiffer, H.; Schindler, M.; Schueler, M.; Seth, M.; Stahlberg, E. A.; Zhao, J. G.; Yabushita, S.; Zhang, C. L.; Barbatti, M.; Matsika, S.; Schuurmann, M.; Yarkony, D. R.; Brozell, S. R.; Beck, E. V.; Blaudeau, J. P.; Ruckenbauer, M.; Sellner, B.; Plasser, F.; Szymczak, J. J. *COLUMBUS, an ab initio electronic structure program*, rel. 7.0, 2017.

https://doi.org/10.1021/jacsau.1c00272
JACS Au 2021, 1, 1647−1655

(42) Head-Gordon, M. Characterizing unpaired electrons from the one-particle density matrix. *Chem. Phys. Lett.* **2003**, *372*, 508−511.
(43) Head-Gordon, M. Reply to comment on 'characterizing unpaired electrons from the one-particle density matrix'. *Chem. Phys. Lett.* **2003**, *380*, 488−489.
(44) Plasser, F.; Bappler, S. A.; Wormit, M.; Dreuw, A. New tools for the systematic analysis and visualization of electronic excitations. II. Applications. *J. Chem. Phys.* **2014**, *141*, 024106.
(45) Plasser, F.; *TheoDORE: A Package for Theoretical Density, Orbital Relaxation, and Exciton Analysis*, ver. 2.0. 2019. http://theodore-qc.sourceforge.net.
(46) Mota, F.; Miller, J. S.; Novoa, J. J. Comparative Analysis of the Multicenter, Long Bond in [TCNE](center dot-) and Phenalenyl Radical Dimers: A Unified Description of Multicenter, Long Bonds. *J. Am. Chem. Soc.* **2009**, *131*, 7699−7707.
(47) Tkatchenko, A.; DiStasio, R. A.; Car, R.; Scheffler, M. Accurate and Efficient Method for Many-Body van der Waals Interactions. *Phys. Rev. Lett.* **2012**, *108*, 236402.
(48) *Amsterdam Density Functional (ADF)*; SCM: Amsterdam, The Netherlands. http://www.scm.com.
(49) Mou, Z.; Uchida, K.; Kubo, T.; Kertesz, M. Evidence of sigma- and pi-Dimerization in a Series of Phenalenyls. *J. Am. Chem. Soc.* **2014**, *136*, 18009−18022.
(50) Small, D.; Rosokha, S. V.; Kochi, J. K.; Head-Gordon, M. Characterizing the dimerizations of phenalenyl radicals by ab initio calculations and spectroscopy: sigma-bond formation versus resonance pi-stabilization. *J. Phys. Chem. A* **2005**, *109*, 11261−11267.
(51) Uchida, K.; Mou, Z. Y.; Kertesz, M.; Kubo, T. Fluxional sigma-Bonds of the 2,5,8-Trimethylphenalenyl Dimer: Direct Observation of the Sixfold sigma-Bond Shift via a pi-Dimer. *J. Am. Chem. Soc.* **2016**, *138*, 4665−4672.
(52) Morita, Y.; Suzuki, S.; Fukui, K.; Nakazawa, S.; Kitagawa, H.; Kishida, H.; Okamoto, H.; Naito, A.; Sekine, A.; Ohashi, Y.; Shiro, M.; Sasaki, K.; Shiomi, D.; Sato, K.; Takui, T.; Nakasuji, K. Thermochromism in an organic crystal based on the coexistence of sigma- and pi-dimers. *Nat. Mater.* **2008**, *7*, 48−51.
(53) Molcanov, K.; Mou, Z. Y.; Kertesz, M.; Kojic-Prodic, B.; Stalke, D.; Demeshko, S.; Santic, A.; Stilinovic, V. Pancake Bonding in pi-Stacked Trimers in a Salt of Tetrachloroquinone Anion. *Chem. - Eur. J.* **2018**, *24*, 8292−8297.
(54) Poduska, A.; Hoffmann, R.; Ienco, A.; Mealli, C. Half-Bonds" in an Unusual Coordinated $S\text{-}4^{2-}$ Rectangle. *Chem. - Asian J.* **2009**, *4*, 302−313.
(55) Zhao, L. L.; von Hopffgarten, M.; Andrada, D. M.; Frenking, G. Energy decomposition analysis. *Wires. Comput. Mol. Sci.* **2018**, *8*, No. e1345.
(56) Zhao, L. L.; Hermann, M.; Schwarz, W. H. E.; Frenking, G. The Lewis electron-pair bonding model: modern energy decomposition analysis. *Nat. Rev. Chem.* **2019**, *3*, 48−63.
(57) Andres, J.; Ayers, P. W.; Boto, R. A.; Carbo-Dorca, R.; Chermette, H.; Cioslowski, J.; Contreras-Garcia, J.; Cooper, D. L.; Frenking, G.; Gatti, C.; Heidar-Zadeh, F.; Joubert, L.; Pendas, A. M.; Matito, E.; Mayer, I.; Misquitta, A. J.; Mo, Y. R.; Pilme, J.; Popelier, P. L. A.; Rahm, M.; RamosCordoba, E.; Salvador, P.; Schwarz, W. H. E.; Shahbazian, S.; Silvi, B.; Sola, M.; Szalewicz, K.; Tognetti, V.; Weinhold, F.; Zins, E. L. Nine questions on energy decomposition analysis. *J. Comput. Chem.* **2019**, *40*, 2248−2283.
(58) Vyboishchikov, S. F.; Krapp, A.; Frenking, G. Two complementary molecular energy decomposition schemes: The Mayer and Ziegler-Rauk methods in comparison. *J. Chem. Phys.* **2008**, *129*, 144111.

https://doi.org/10.1021/jacsau.1c00272
JACS Au 2021, 1, 1647−1655